

# Supporting Information

Sharma et al. 10.1073/pnas.1107087108

## SI Materials and Methods

**Flow Cytometry.** The antibodies to CD8 (53-6.7), CD4 (RM4-5), CD62 ligand (CD62L) (MEL-14), CD44 (IM7), IFN $\gamma$ , TNF $\alpha$ , IL-2, and CD103 (2E7) were purchased from BD Bioscience. Phycoerytherin- and allophycocyanin-conjugated Tim-3 antibodies were purchased from R&D Systems. Intranuclear FoxP3 staining (E-Bioscience) was performed according to the instructions. Cell suspensions were blocked with anti-mouse CD16/32 and then incubated with specific antibodies or isotypes for 30 min at 4 °C. The antibody-stained cells were acquired with a FACS Calibur

(BD Biosciences) and the data were analyzed using the FlowJo software (Tree Star).

**Adoptive Transfers.** Splenocytes from WT or G9KO (both Thy1.2)  $\times 31$  immune mice were enriched (Miltenyi Biotech kit) for CD8 T cells and then titrated for  $10^4$  NPtet $^+$  CD8 T cells and transferred into Thy1.1 C57BL/6 animals. Alternatively  $10^4$  NPtet $^+$  CD8 T from B6Thy1.1 ( $\times 31$  immune) mice were transferred into Thy1.2 C57BL/6 WT or G9KO animals. At 24 h posttransfer, recipient animals were infected with 8,000 EID $_{50}$  pfu of IAV PR8. At 8 d postchallenge, CD8 T-cell analysis was performed.

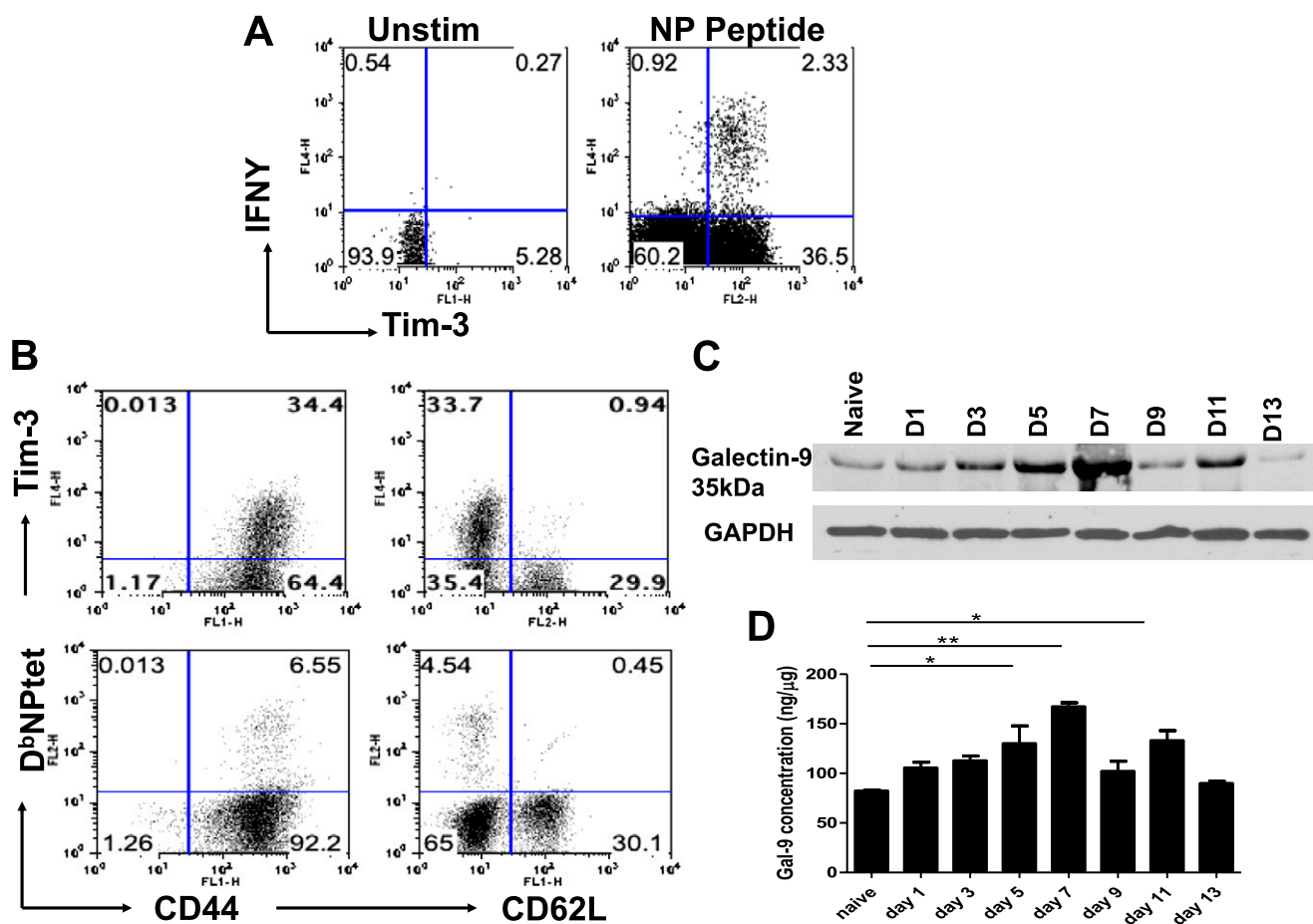


**Fig. S1.** Activated cells express Tim-3 and Gal-9 levels are up-regulated in lungs after IAV infection. At different time points after infection, BAL and spleen cells ( $n = 3$ ) isolated at each time point were analyzed flow cytometrically for Tim-3 expression on IAV-specific CD8 T cells. BAL samples from three mice were pooled. (A) FACS plots showing Tim-3 $^+$ IFN $\gamma$  $^+$  CD8 T cells at day 10 p.i. in the BAL fluid of WT animals. (B) Coexpression of Tim-3 (Upper) and D $^b$ NPtet $^+$  (Lower) with CD44 and CD62L in BAL of WT mice at day 8 p.i. is shown by representative FACS plots. (C) Immunoblots showing Gal-9 expression in the lung homogenates from naïve and IAV-infected mice at different time points post infection. (D) Gal-9 concentrations as measured by sandwich ELISA using anti-Gal-9 mAb in the lung homogenates is shown. Numbers in the quadrants indicate percent of each subset. Data are representative of three independent experiments.

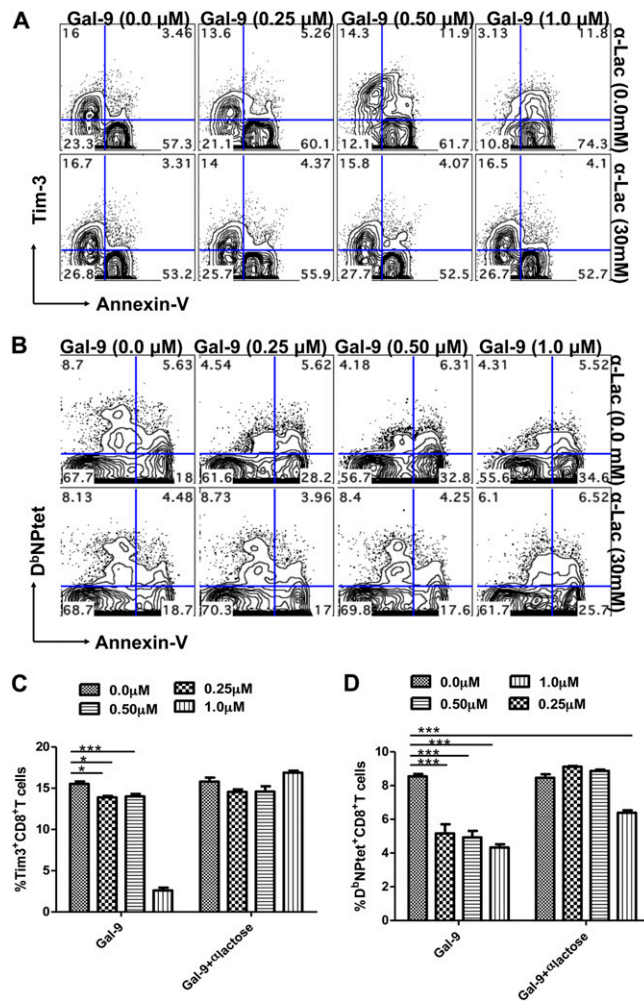


**Fig. S2.** Galectin-9 induces apoptosis of IAV NP tetramer-specific and Tim-3<sup>+</sup> CD8 T cells in vitro. Ex vivo apoptosis assay was performed with splenocytes isolated at 10 days postinfection from IAV-infected animals as described previously (1). Briefly splenocytes were incubated for 5 h with varying concentrations of galectin-9 in the absence or presence of α-lactose. The experiments were repeated multiple times with similar results. (A) Representative FACS plots showing the expression of Tim-3 and annexin-V on gated CD8 T cells under indicated incubation conditions. (B) Representative FACS plots showing the expression of NPtet and annexin-V on gated CD8 T cells under indicated incubation conditions. (C) Bar diagram shows the percentage of Tim-3<sup>+</sup> CD8 T cells as calculated from A (with triplicate wells). (D) Bar diagram shows the percentage of NPtet<sup>+</sup> CD8 T cells as calculated from B. Statistical analysis was done by two-way ANOVA with Bonferroni post hoc settings.

1. Sehrawat S, et al. (2010) Galectin-9/TIM-3 interaction regulates virus-specific primary and memory CD8 T cell response. *PLoS Pathog* 6:e1000882.

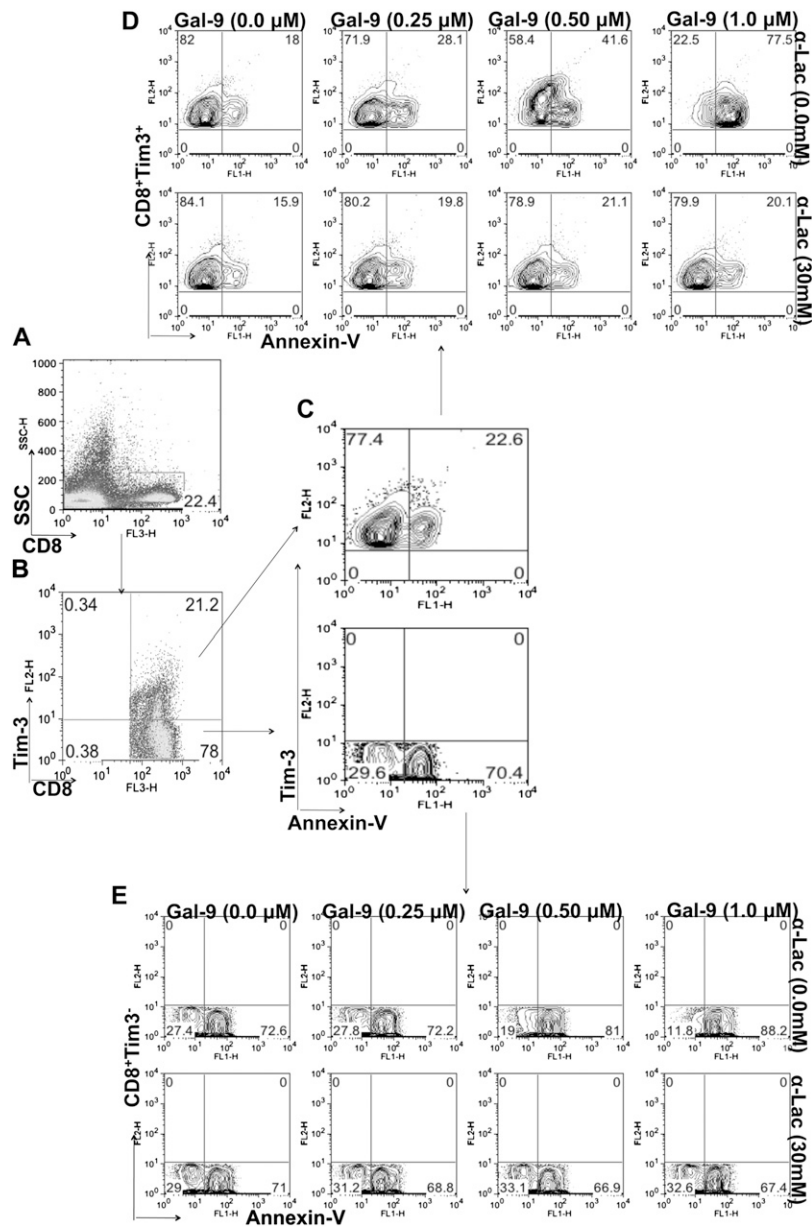


**Fig. S3.** Gating strategy to depict preferential apoptosis of Tim-3<sup>+</sup> CD8T cells upon Galectin-9 exposure. (A) Representative FACS plots showing gated CD8T cells from the cultures in an ex vivo apoptosis assay. (B) Tim-3<sup>+</sup> and Tim-3<sup>-</sup> CD8T cells are shown by representative FACS plot. (C) FACS plots depicting Tim-3<sup>+</sup> annexinV<sup>+</sup> (Upper) and Tim-3<sup>-</sup> annexin V<sup>+</sup> CD8 T cells (Lower). (D) Representative FACS plots showing the expression of annexin-V on gated Tim-3<sup>+</sup> CD8 T cells under indicated incubation conditions. (E) Representative FACS plots showing the expression of annexin-V on gated Tim-3<sup>-</sup> CD8 T cells under indicated incubation conditions.

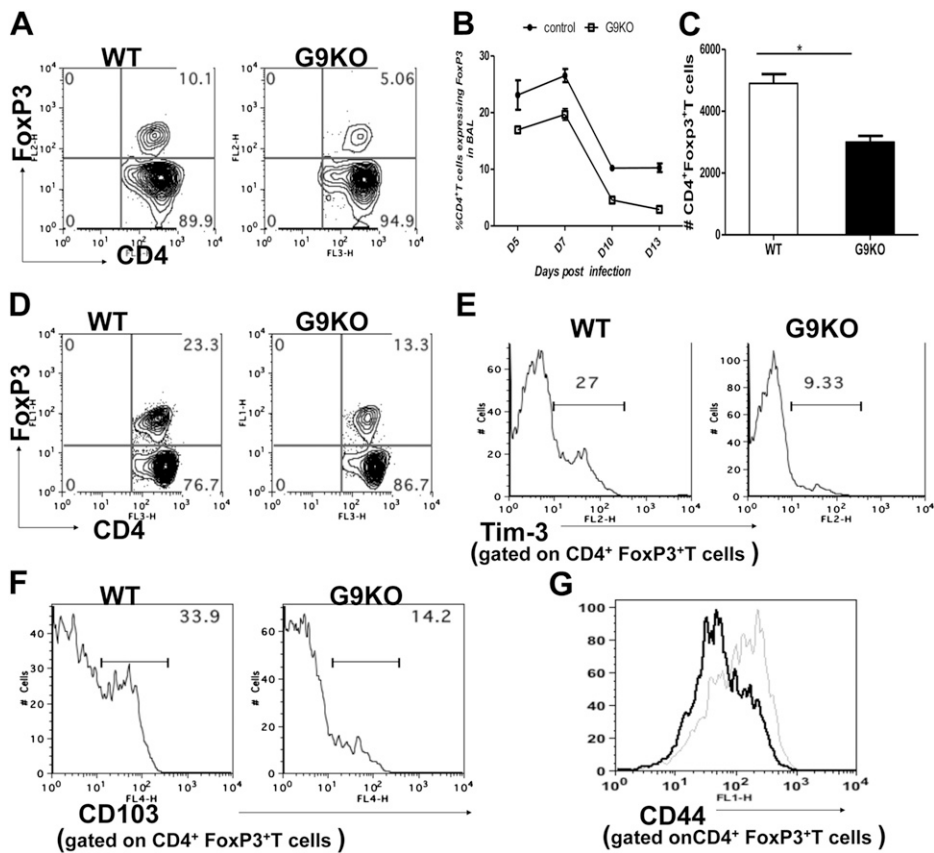


**Fig. 54.** Characterization of  $CD4^+FoxP3^+$  regulatory T cells from WT and G9KO mice. C57BL/6 and G9KO animals were infected intranasally with 5,000 EID<sub>50</sub>. BAL samples from three mice were pooled and spleens from individual mice were stained for FoxP3. Representative FACS plots show the frequencies of FoxP3<sup>+</sup> Tregs in the BAL (A) and spleens (D) of WT and G9KO animals at day 10 p.i. The kinetics of Treg frequencies at indicated timepoints p.i. (B) and their absolute numbers at day 10 p.i. (C) in the BAL fluid of WT and G9KO are shown. Histograms show the expression of Tim-3 (E), CD103 (F), and CD44 (WT, light line) and (G9KO, dark line) (G) on FoxP3<sup>+</sup> Tregs isolated from the spleens of WT and G9KO animals at day 10 p.i.

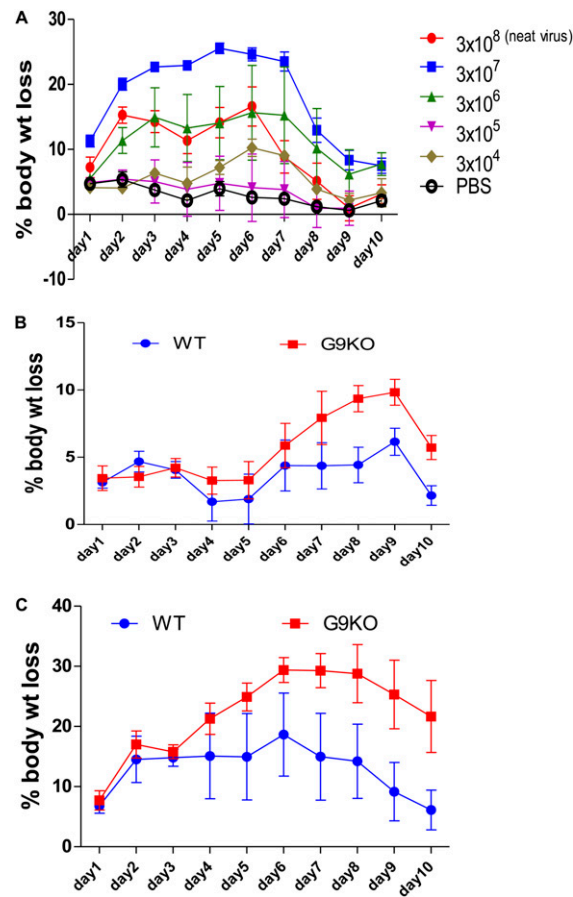


**Fig. 55.** Outcome of infection with IAV HKx31. WT mice were inoculated with IAV HKx31 ( $10^8$ ,  $10^7$ ,  $10^6$ ,  $10^5$ ,  $10^4$  EID<sub>50</sub> or PBS). (A) Body weight of WT mice after infection was determined daily and expressed as the percentage of the body weight lost following infection. (B) Percentage of body weight-loss comparison between the WT and G9KO mice infected with 5,000 EID<sub>50</sub> intranasally (*i/n*) over a period of 10 d. (C) Percentage of body weight-loss comparison between WT and G9KO mice infected with  $5 \times 10^7$  EID<sub>50</sub> *i/n* over a period of 10 d. The data are representative of five to six mice per group.

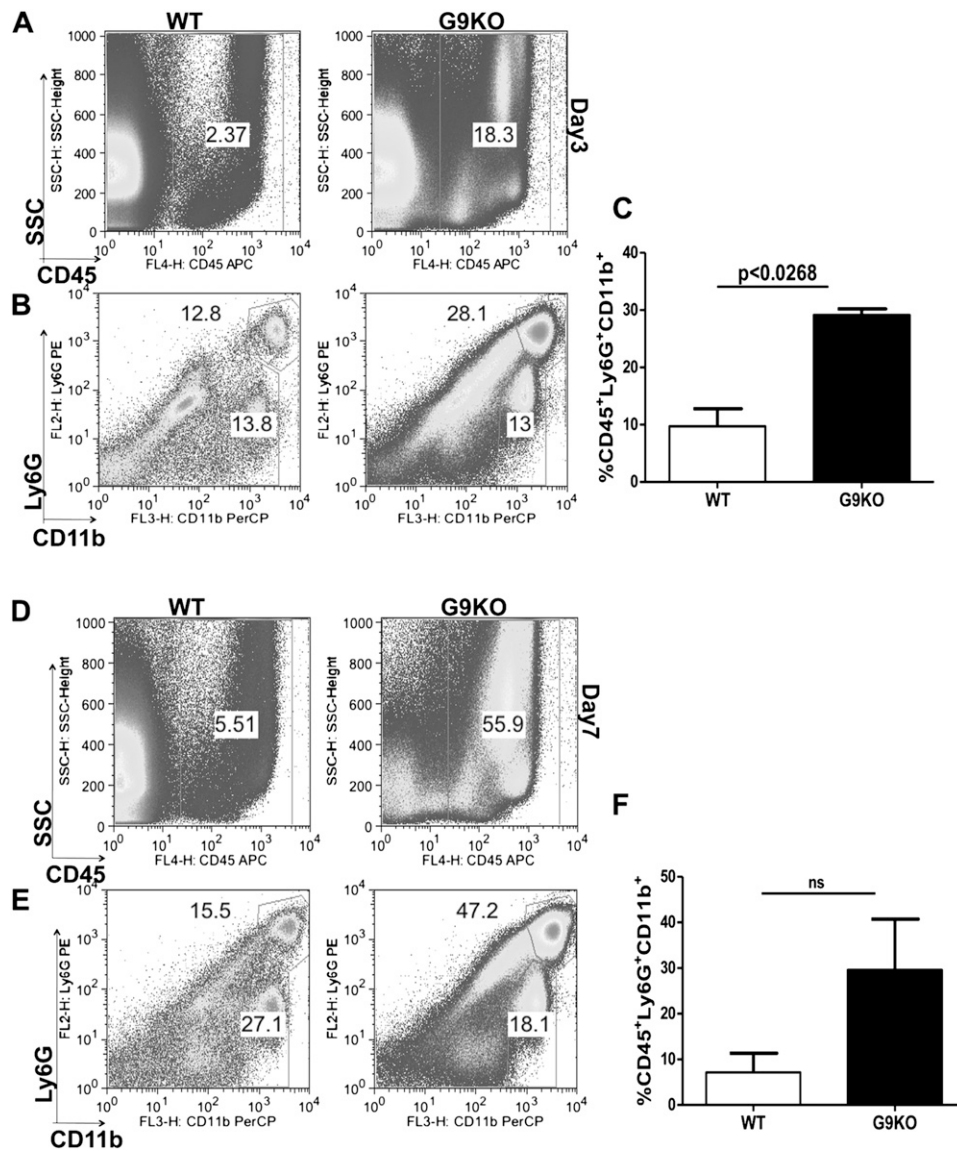
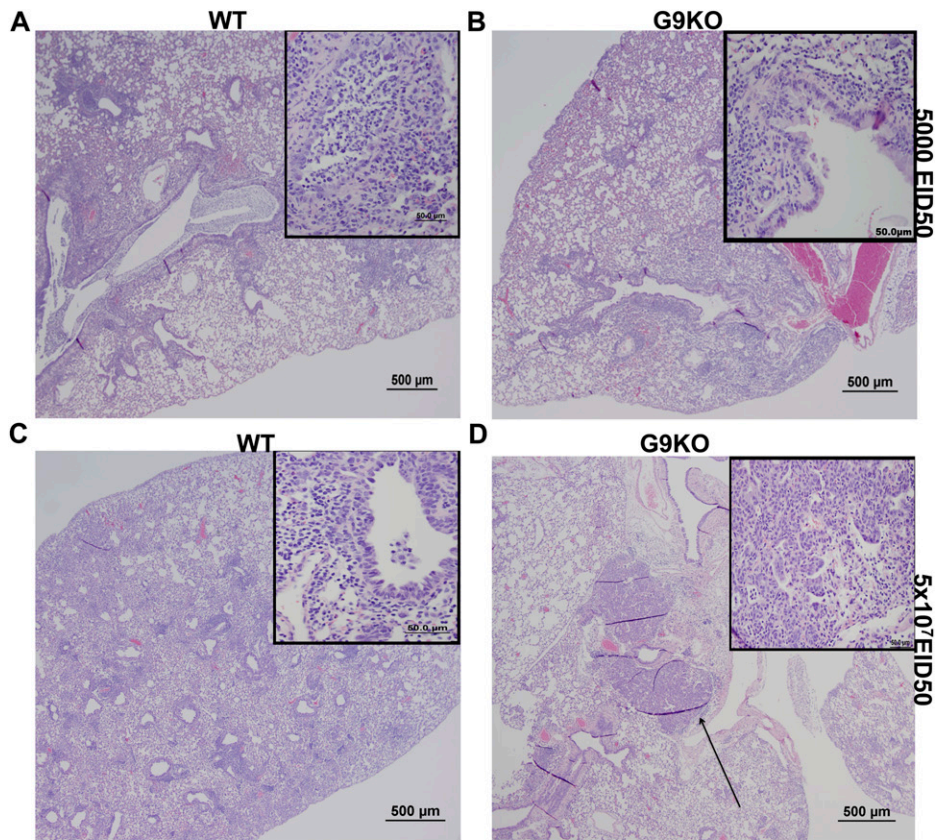


**Fig. 56.** Cells obtained from bronchoalveolar lavage (BAL) were stained for CD45<sup>+</sup> (pan leukocyte marker) and CD45<sup>+</sup>CD11b<sup>+</sup>Ly6G<sup>+</sup> (neutrophils) and FACS analysis performed at day 3 (A and B) and day 7 (D and E) in WT and G9KO mice. Bar graphs representing % CD45<sup>+</sup>CD11b<sup>+</sup>Ly6G<sup>+</sup> (neutrophils) at day 3 p.i. (C) and day 7 p.i. (F) is shown. Experiments were repeated multiple times and the data are representative of pooled BAL samples from three mice. Statistical analysis was done by Student's *t* test and error bars represent SEM.





**E**

		%Parenchyma involved	PMN# (Average/40x field)	Remarks
WT	Day 3	0%	0	Normal lung, no recognizable pathological changes
	Day 7	1-4	2-4	Mild multifocal broncho-interstitial pneumonia
	Day 9	21-30%	4-30	Moderate to marked multifocal broncho-interstitial pneumonia, primarily mononuclear lymphocytic infiltrates with lesser number of macrophages, scattered parenchymal/infiltrative individual cell necrosis and degeneration
G9KO	Day 3	4%	0-5	Mild, regionally limited, multifocal broncho-interstitial pneumonia
	Day 7	4-5%	5-7	Mild multifocal broncho-interstitial pneumonia
	Day 9	10-20%	2-50	Moderate multifocal broncho-interstitial pneumonia, primarily mononuclear lymphocytic infiltrates with lesser numbers of macrophages, occasional foci of intense neutrophilic infiltrates, moderate scattered parenchymal/infiltrative individual cell necrosis/apoptosis

**Fig. S7.** Histopathology. The lungs of mice infected with 5,000 or  $5 \times 10^7$  EID<sub>50</sub> of virus were harvested at indicated timepoints postinfection, washed in PBS, fixed in 10% neutral buffered formalin, and embedded in paraffin wax. Sections (5 mm) were stained with hematoxylin and eosin and microscopically reviewed. H&E sections from WT (A) and G9KO (B) animals infected with 5,000 EID<sub>50</sub> of IAV  $\times 31$  at day 9 p.i. are shown. Representative H&E sections from WT (C) and G9KO (D) animals infected with  $5 \times 10^7$  EID<sub>50</sub> of IAV  $\times 31$  at day 10 p.i. are shown. The section blocks in the *Upper Right* corner represent the 40 $\times$  magnification. The overall lung readouts ( $n = 3$  mice at each timepoint/group infected with  $\times 31$  5,000 EID<sub>50</sub>) are indicated as a table (E).

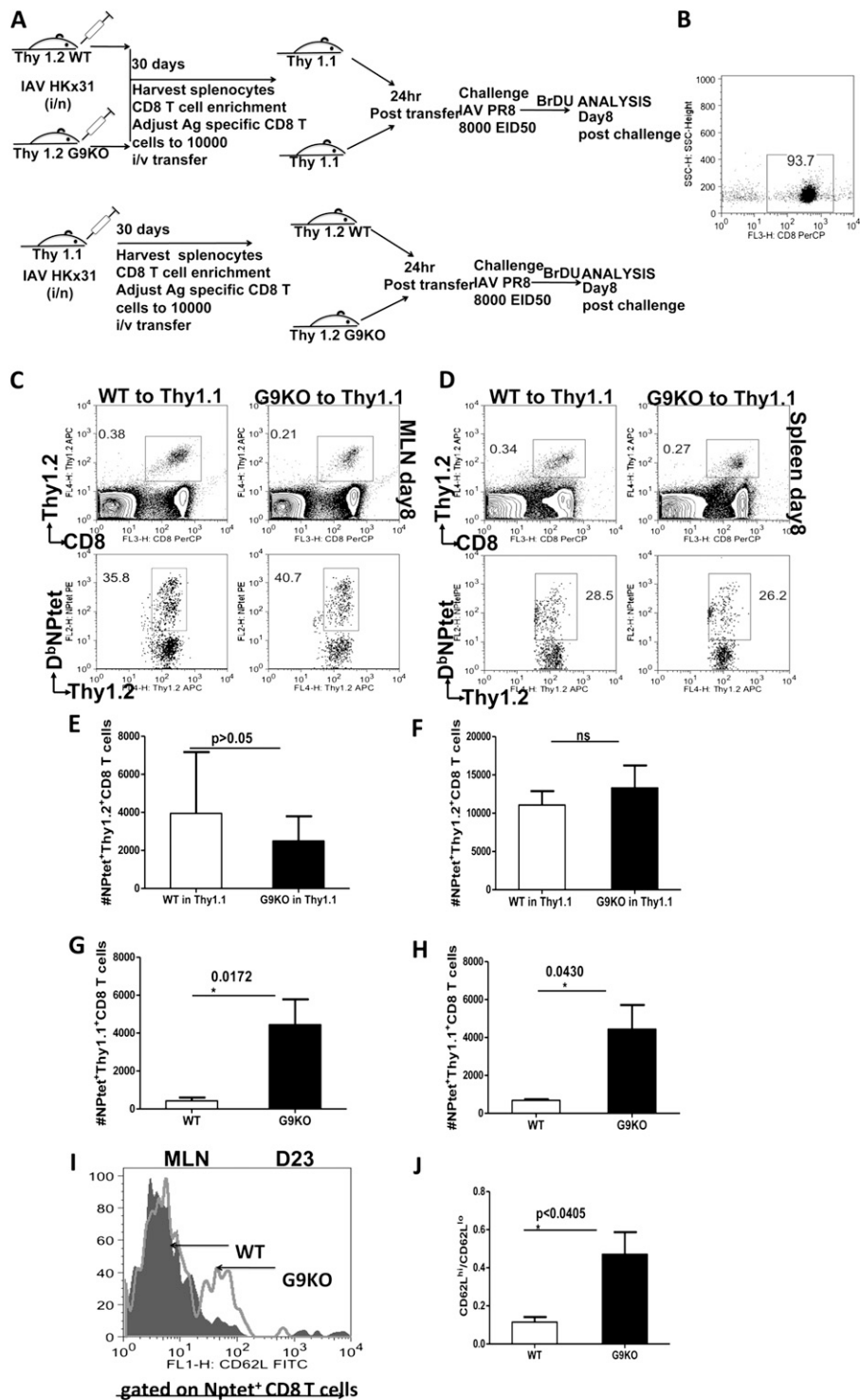


**Fig. S8.** Adoptive transfer of memory CD8 T cells. Splenocytes from either WT or G9KO (both Thy1.2) HKx31 immune mice (mice were held for at least 1 mo following infection with IAV HKx31 i/n) were enriched for CD8T cells using Miltenyi Biotech (CD8T cell isolation) kit. Around 93–94% pure CD8T cells were obtained in the enriched CD8T cell population. The enriched CD8T cells were then titrated for equal number of NP tetramer-specific CD8T cells and  $1 \times 10^4$  antigen-specific CD8T cells were transferred in B6 Thy1.1 mice ( $n = 4$ ). Alternatively splenocytes from B6 Thy1.1 HKx31 immune mice (mice were held for at least 1 mo following infection with IAV HKx31 i/n) were enriched for CD8T, and equal number of NP tetramer-specific CD8T ( $1 \times 10^4$ ) cells were transferred in WT or G9KO mice ( $n = 4$ ). Twenty-four hours posttransfer, the recipients were challenged with 8,000 EID<sub>50</sub> of heterologous IAV (PR8). (A) Diagrammatic depiction of the scheme for adoptive transfer experiments. (B) Representative FACS plots for enriched CD8T cell population. FACS plots show the frequencies of donor Thy1.2<sup>+</sup>CD8<sup>+</sup> (C, Upper) and NPtet<sup>+</sup>Thy1.2<sup>+</sup>CD8<sup>+</sup> (C, Lower) WT or G9KO cells in the MLN (C), and spleen (D) of Thy1.1 animals at 8 d p.i. Absolute numbers of the donor NPtet<sup>+</sup>Thy1.2<sup>+</sup>CD8<sup>+</sup>T cells of WT or G9KO in the MLN (E) and spleens (F) of the recipients are shown. Absolute numbers of the donor NPtet<sup>+</sup>Thy1.1<sup>+</sup>CD8<sup>+</sup>T WT or G9KO cells in the MLN (G) and spleens (H) of the recipients are shown. The experiments were repeated two times. Statistical analysis was done by Student's *t* test and the error bars represent SEM. (I) Representative histograms showing CD62L expression by NPtet<sup>+</sup> CD8 T cells in the MLNs of WT and G9KO animals at day 23 p.i. (J) Bar graphs represent the ratios of CD62L<sup>hi</sup>/CD62L<sup>lo</sup> of NPtet<sup>+</sup> CD8 T cells in the MLN of WT and G9KO animals at day 23 p.i.



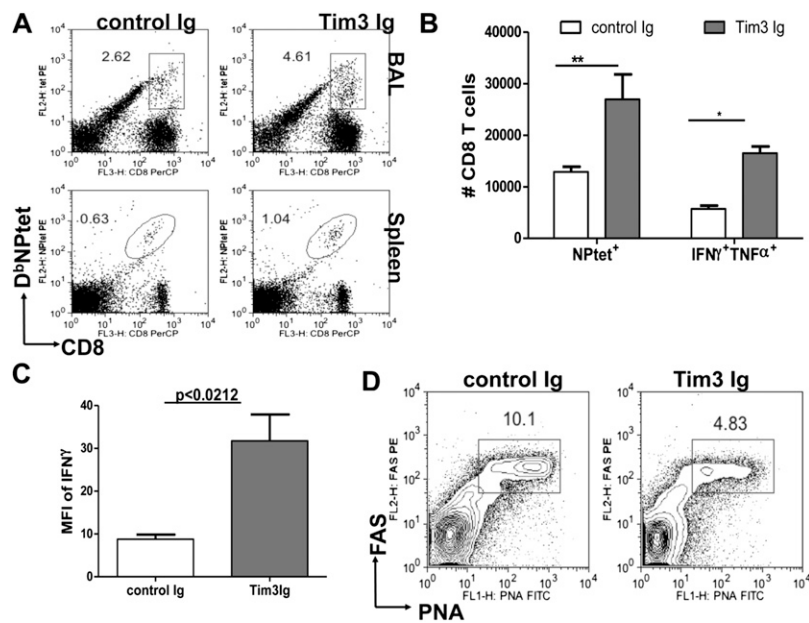


**Fig. S9.** Administration of Tim-3 fusion protein in mice at later stages post IAV infection enhances the magnitude and quality of IAV-specific CD8 T cell responses. IAV-infected C57BL/6 animals were treated with 100  $\mu$ g of Tim-3 fusion protein (per mouse) from day 4 postinfection at alternate days until day 9 p.i., and 12 h after the last treatment the animals were killed. Frequencies of NPtet<sup>+</sup> CD8 T cells (**A**) isolated from the BAL (*Upper*) and spleen (*Lower*) of Tim-3 fusion protein-treated and control animals are shown. (**B**) Absolute numbers of NPtet<sup>+</sup>, IFN $\gamma$ <sup>+</sup>TNF $\alpha$ <sup>+</sup> CD8 T cells in the BAL. (**C**) MFI of IFN $\gamma$  in Tim-3 Ig and control animals. (**D**) Representative FACS plots showing frequencies of CD3<sup>+</sup>B220<sup>+</sup>PNA<sup>+</sup>FAS<sup>+</sup> germinal center B cells in the mediastinal lymph node (MLN) of Tim-3 Ig and control Ig-treated mice at day 10 p.i. Data are representative of two independent experiments with three mice per group. Error bars represent SEM.